J Solid State Electrochem (2005) 9: 717–731
DOI 10.1007/s10008-005-0693-3

REVIEW

Paul J. Low · Rachel L. Roberts
Richard L. Cordiner · František Hartl

# Electrochemical studies of bi- and polymetallic complexes featuring acetylide based bridging ligands

Received: 19 October 2004 / Revised: 6 January 2005 / Accepted: 24 January 2005 / Published online: 28 September 2005


**Abstract** Acetylide-based bridging ligands have been widely used in the preparation of complexes that display a degree of electronic interaction between metal-based redox groups located at the ligand termini. The electrochemical response of these systems has been selectively reviewed, with a focus on the variation in properties that accompany changes in the structure of the bridging ligand and the nature of the metal groups.

**Keywords** Acetylide · Metal complex · Mixed-valence chemistry

## Introduction

Mixed-valence complexes and intra molecular electron transfer processes have been, and continue to be, a focus of fundamental and applied research [1–8]. The interest in these systems, which contain examples of an element in more than one oxidation (or valence) state, arise from the role such systems play in biological systems, their use as probes for inner-sphere electron transfer reactions and tests of theory, and most recently for their potential as components in molecular scale electronic devices.

Many mixed-valence materials of contemporary interest feature a common $[L_xM]$-B-$[ML_x]$ structure, in which two (redox-active) metal fragments $ML_x$ featuring a metal centre in oxidation state *n*, are linked by some bridging ligand, B. The mixed valence state is generated by one-electron oxidation (or reduction) of the assembly (Scheme 1). Through investigations of the roles played by the structure of the bridging ligand and the nature of the metal and supporting ligands structure on the extent of delocalisation of the unpaired electron through the molecular assembly we, and others, hope to establish the design rules for next generation molecular electronic and magnetic materials.

The volume of literature is such that we cannot comprehensively review mixed-valence chemistry, or the theoretical treatments used to analyse them, in this contribution. Rather, we shall take an overview of the works featuring the acetylene-based bridging ligands of particular interest to this research group, with special attention given to the most recent results from us and others [9–15]. We hope that in doing so we will provide a ready point of entry to the field for those with an interest in organometallic chemistry and the electrochemical properties of the systems in question, and illustrate the electrochemical techniques being employed in the generation and study of these complexes.[1]

## Mixed valence compounds: a summary and overview

The classification system and the terminology introduced by Robin and Day [2] is widely used in the description of mixed-valence systems. The Robin and Day system distinguishes three general classes of mixed valence compound: Class I, in which the interactions between sites containing the redox-active element are negligible either because of the great distance between them, or because the local environment of each site is very different; Class II, in which the redox centres are in

Presented at the 3rd Chianti Electrochemistry Meeting, July 3–9, 2004, Certosa die Pontignano, Italy

P. J. Low (✉) · R. L. Roberts · R. L. Cordiner
Department of Chemistry, University of Durham,
South Rd, Durham, DH1 3LE, UK
E-mail: p.j.low@durham.ac.uk
Fax: +44-191-3844737

F. Hartl
Van't Hoff Institute for Molecular Sciences,
University of Amsterdam, Nieuwe Achtergracht 166, 1018 WV Amsterdam, The Netherlands

[1] Given the large range of solvents, electrolytes and reference electrodes used in different research laboratories, comparison of data between groups can be complicated. Throughout the text we quote electrochemical potentials as given in the original literature, together with an indication of the conditions and any internal reference couple employed.

**Scheme 1**

$$[M^{(n)}L_x]{-}B{-}[M^{(n)}L_x] \underset{+e}{\overset{-e}{\rightleftharpoons}} [M^{(n+1)}L_x]{-}B{-}[M^{(n)}L_x] \rightleftharpoons [M^{(n)}L_x]{-}B{-}[M^{(n+1)}L_x]$$

similar local environments, with moderate coupling between them permitting electron exchange, and in addition to properties arising from the electron transfer process have identifiable independent character arising from localisation (or trapping) of the unpaired electron; and Class III, in which the redox centres are so strongly coupled that the odd-electron is delocalised and only a single, average valence state can be assigned to the two centres. Strictly speaking, Class III compounds are not "mixed-valence", but perhaps better described as "valence averaged" species, with unique characteristics that cannot be assigned to either individual oxidation state.

The thermodynamic stability of the mixed-valence state can be readily calculated from electrochemical data. The comproportionation (equilibrium) constant, $K_c$, for the reaction shown in Scheme 2 is given by $K_c = e^{\frac{\Delta EF}{RT}}$, where $\Delta E$ is the difference in oxidation potentials associated with the first and second oxidation of the parent $[L_xM]$-B-$[ML_x]$ species and ranges from $K_c \sim 4$ (in the statistical limit) for the most weakly coupled systems to $>10^{13}$ for the most strongly coupled (Class III) systems. However, it must be emphasised that $K_c$ is a thermodynamic parameter and should probably not be used in isolation when determining the nature (class) of a mixed-valence complex. Nevertheless, the magnitude of $\Delta E$ has often been taken as an indication of the degree of interaction between identical redox sites [16].

The determination of the nature and magnitude of the electronic coupling between redox sites in mixed-valence complexes has been a subject of study for decades and continues to pose many fundamental and challenging problems [5, 17–20]. In a Class II mixed-valence complex of the type shown in Scheme 1, electron transfer between the two sites M can be induced thermally or photochemically. In his classic work, Hush developed the theoretical treatments which both predicted the occurrence of this metal-metal charge transfer (MMCT, or intervalence charge transfer IVCT) band and allowed thermal parameters to be extracted from analysis of the energy and shape of this optical absorption band. In the context of this micro-review it is only appropriate to note the key conclusions and relationships relating the optical properties of mixed-valence

$$[M^{(n)}L_x]{-}B{-}[M^{(n)}L_x] \; + [M^{(n+1)}L_x]{-}B{-}[M^{(n+1)}L_x]$$
$$\Big\Updownarrow K_c$$
$$2 \quad [M^{(n+1)}L_x]{-}B{-}[M^{(n)}L_x]$$

**Scheme 2**

species that are most commonly used by the inorganic community in the analysis of their data.

In the case of a symmetric complex, the rate constant for the intramolecular electron transfer process, $k_{th}$, can be obtained from

$$k_{th} = \kappa \nu_n e^{\left(\frac{-\Delta G^*_{th}}{RT}\right)}, \tag{1}$$

where $\kappa$ is the adiabatic factor, and $\nu_n$ is the nuclear frequency factor (ca. $1–10\times10^{12}$ $s^{-1}$ at 25 °C).

Although the two states before and after electron transfer are indistinguishable, and overall for this process $\Delta G^0 = 0$, there is an activation barrier $\Delta G^*_{th}$ to the electron exchange process imposed by the different equilibrium geometries (inner and outer sphere, or metal–ligand lengths and solvation shells) of $M^{(n)}$ $L_x$ and $M^{(n+1)}$ $L_x$ and Franck–Condon factors. Electron transfer can occur without prior rearrangement of the complex upon absorption of light of the appropriate energy, $E_{op}$. For a Class II system, $\Delta G^*_{th}$ is given by

$$\Delta G^*_{th} = \left(\frac{\lambda}{4} - V_{ab}\right) + \frac{V_{ab}^2}{\lambda} \tag{2a}$$

which in the case of very weakly coupled systems simplifies to

$$E_{op} = \lambda = h\nu = 4\Delta G^*_{th} \tag{2b}$$

and the bandwidth at half-height $\Delta\bar{\nu}_{1/2}$ ($cm^{-1}$) of the optical transition is related to the energy of the transition $\bar{\nu}_{max}$ by

$$\Delta\bar{\nu}_{1/2} = \sqrt{2310\bar{\nu}_{max}}. \tag{3}$$

A rough rule of thumb assigns mixed-valence classes based on the comparison of the observed ($\Delta\bar{\nu}_{1/2(obs)}$) and calculated ($\Delta\bar{\nu}_{1/2}$) half-height bandwidths. The band shape of the "IVCT" band in strongly coupled systems has been a topic of considerable recent debate, as the ground state potential energy surfaces are no longer parabolic in shape, leading to a "cut-off" of the absorption band on the low energy side at $h\nu = 2V_{ab}$. Complexes with asymmetric (non-Gaussian) shaped bands that are significantly narrower than the Hush relationship predicts are assumed to belong to Class III [18, 21].

The IVCT band also allows extraction of the electronic coupling term $V_{ab}$ (also written $H_{ab}$) via

$$V_{ab} = \frac{0.0205}{r}\sqrt{\varepsilon_{max}\Delta\bar{\nu}_{1/2}\bar{\nu}_{max}}, \tag{4}$$

where $\epsilon_{max}$ is the molar absorption coefficient of the IVCT band, and $r$ is the intramolecular electron transfer distance (in Å). An alternative, quantum mechanical expression for $V_{ab}$ which makes no implicit assumption of the band-shape is

$$V_{ab} = \frac{\mu_{eg}}{er}\bar{\nu}_{max}, \quad (5)$$

where $\mu_{eg}$ (in C m) is the transition dipole moment between the ground and excited states and can be calculated (in Debye, 1 D = $3.336\times10^{-30}$ C m) from the integrated area of the IVCT band through

$$\mu_{eg} = 0.09584\sqrt{\frac{\int \varepsilon(\bar{\nu})d\bar{\nu}}{\bar{\nu}_{max}}}. \quad (6)$$

While $r$ is often assumed to be the metal–metal separation, estimates of $r$ can be difficult when the redox-active orbitals are significantly delocalised over several atomic sites [22–25]. Curtis and co-workers [26] have described an alternative, electrochemical approach for the measurement of the coupling parameter, although this method requires data from a significant number of closely related complexes and Hush style analysis of IVCT band shape has dominated the more recent organometallic literature. DFT methods have also been applied recently to the calculation of the intramolecular electron transfer distance and $V_{ab}$ in triarylamine based mixed-valence compounds [25].

Another measure of the extent of interaction between the two redox sites often used in the earlier literature is the delocalisation coefficient, or a ground state delocalisation parameter $\alpha^2$, which is proportional to the amount of time spent by an electron at a given site [27]. The parameter is calculated from the spectroscopic data through the following relationships

$$V_{ab} = \bar{\nu}_{max}\alpha = 2.05\times10^{-2}\left(\frac{\bar{\nu}_{max}}{r}\right)\left(\frac{\varepsilon_{max}\Delta\bar{\nu}_{1/2}}{\bar{\nu}_{max}}\right)^{1/2} \quad (7)$$

$$\alpha^2 = \frac{(4.2\times10^{-4})\varepsilon\Delta\bar{\nu}_{1/2}}{\nu_{max}r^2}. \quad (8)$$

In the case of delocalised (Class III) systems, $V_{ab}$ is simply related to the transition energy by the following relationship

$$E_{op} = \bar{\nu}_{max} = 2V_{ab}. \quad (9)$$

Many of the terms used in the description of localised Class II systems, such as "IVCT" and even "mixed-valence", are rather misleading when directly applied to Class III systems. The term "charge resonance band" may be a more appropriate descriptive term [24, 28].

## $C_n$ bridged species

The electrochemical response of bimetallic species bridged by polycarbon fragments and related ligands derived from polyynes was comprehensively reviewed recently [11, 29]. However, these reviews explicitly omitted ferrocene derivatives, and we take the opportunity to summarise the redox chemistry associated with polycarbon bridged ferrocenes in this section.

Diferrocenylacetylene, FcC ≡ CFc (**1/1**), the first member of the simplest family of polyacetylide-bridged bis(ferrocenes), $Fc(C\equiv C)_nFc$ (**1/n**), displays two reversible oxidation waves, separated by up to 190 mV, which has been taken as measure of moderate degree of interaction between the ferrocene centres. With the other members of the series, the value of $\Delta E$ decreases sharply with increasing chain length becoming a single, two electron event in the octatetrayne (n = 4) (Table 1). The electron-rich derivative 1,4-bis(octamethylferrocenyl)-buta-1,3-diyne exhibited a slightly greater $\Delta E$ (150 mV) than **1/2** [35].

In early work, Cowan and co-workers [31, 36] observed low-intensity, low energy absorption bands in the mixed-valence complexes $[\mathbf{1/1}]^+$ ($\lambda_{max}$ = 1,560 nm,

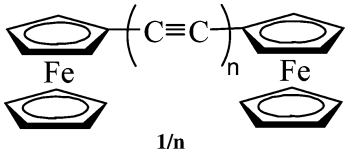


**1/n**

**Structure 1**

**Table 1** The electrochemical properties of bis(ferrocenyl)polyynes **1/n**

| *n* | $E_{1/2}$ (1) | $E_{1/2}$ (2) | $\Delta E$ | Conditions | References |
|---|---|---|---|---|---|
| 1 | −0.11 | 0.08 | 0.19 | 0.1 M $NBu_4ClO_4$ in $CH_2Cl_2$, 100 mV/s, vs. $FcH/FcH^+$ | [30] |
| | 0.625 | 0.755 | 0.130 | 0.2 M $NBu_4BF_4$ in $CH_2Cl_2$, 100 mV/s, vs. SCE | [31] |
| 2 | 0.14 | 0.23 | 0.09 | 0.1 M $NBu_4ClO_4$ in $CH_2Cl_2$, 100 mV/s, vs. $FcH/FcH^+$ | [30] |
| | 0.58 | 0.68 | 0.100 | 0.2 M $NBu_4BF_4$ in $CH_2Cl_2$, 100 mV/s, vs. SCE | [31] |
| | 0.486 | 0.586 | 0.100 | 0.1 M $NBu_4PF_6$ in 1:1 $CH_2Cl_2$:NCMe, vs. Ag/AgCl, 100 mV/s | [32] |
| | 0.58 | 0.69 | 0.11 | 0.1 M $NBu_4PF_6$ in $CH_2Cl_2$, vs decamethylferrocene [0.0765 V vs. SCE] | [33] |
| 3 | | | 0.060 | | [33] |
| 4 | 0.601 | | | 0.1 M $NBu_4PF_6$ in 1:1 $CH_2Cl_2$:NCMe, vs. Ag/AgCl | [34] |
| 6 | 0.652 | | | 0.1 M $NBu_4PF_6$ in 1:1 $CH_2Cl_2$:NCMe, vs. Ag/AgCl | [34] |

**Structure 2**

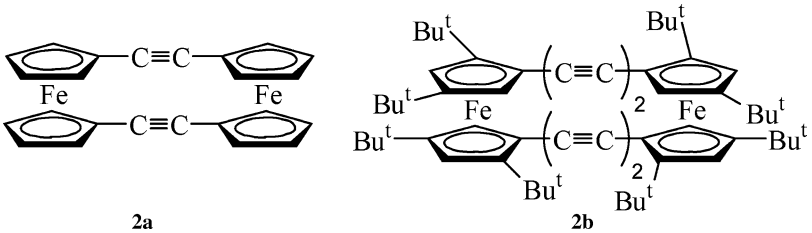


**2a** **2b**

$\epsilon = 670\ M^{-1}\ cm^{-1}$) and $[\mathbf{1/2}]^+$ ($\lambda_{max} = 1{,}180$ nm, $\epsilon = 570\ M^{-1}\ cm^{-1}$), which were not present in either the neutral or dicationic derivatives and were assigned to the Hush-type IVCT bands, and subsequently studied in some detail [37–39]. The doubly bridged species **2a** and **2b** both exhibit two sequential one electron oxidation events with significantly greater separation in the half-wave potentials than the singly bridged analogues ($\Delta E = 0.355$ V **2a**; 0.25 V **2b**). In addition, the mixed-valence cation derived from **2a** gave rise to a much lower energy NIR absorption band with larger molar absorption coefficient ($\lambda_{max} = 1{,}760$ nm; $\epsilon = 3{,}100\ M^{-1}\ cm^{-1}$) than **1/1**, and these doubly bridged species are assumed to be more strongly coupled than the singly bridged derivatives [31, 40]. Cyclic derivatives have also been prepared and electrochemical properties reported in brief [41].

## Transition metal cluster bridged species

The carbon chain in **1/2**, **1/4** and **1/6** has been elaborated through reaction with osmium, ruthenium and cobalt clusters to afford a range of metallo-carbon cluster species featuring pendant ferrocenyl moieties [42–55]. In the case of products in which the ferrocene moieties are found in identical chemical environments and the difference in oxidation potential can be related to the interactions between the redox sites rather than chemical differences, coordination of the polycarbon chain resulted in a decrease in the separation of the oxidation potentials compared with the parent species **1/n**. However, in the case of **3** the redox processes associated with oxidation of the ferrocenyl moieties are separated by 0.184 V, significantly larger than $\Delta E$ of diferrocenylbutadiyne (**1/2**) (0.100 V). The enhanced interaction between the ferrocenyl moieties is thought to be due to mixing of the Os and alkyne carbon orbitals

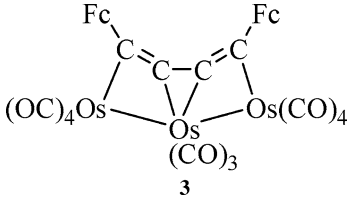


**3**

**Structure 3**

increasing the dehydrobutadiene (C = C = C = C) character of the bridge [32].

The coordination of $Co_2(CO)_6$ moieties to the C ≡ C bridges generally serves to decrease interactions between ferrocenyl groups along the length of the $C_n$ bridge, although the redox processes are complicated by rapid, subsequent chemical processes [56]. In some cases coordination of a $Co_2(CO)_4$(dppm) moiety to the C ≡ C fragments of the bridge can lead to an increase in $\Delta E$ associated with oxidation of the remote ferrocenyl probe groups, but the effect is generally small [33, 57]. There are no electrochemically detectable interactions between $Re(CO)_3$(NN) fragments (NN = 2,2'-bipyridine based ligands) mediated by the $Cu_3(\mu_3\text{-}\eta^1\text{-}C \equiv CC_6R_4C \equiv C)(LL)_3$ bridge. Rather the complex exhibits $Cu_3$ centred oxidation and $Re(CO)_3$(NN) centred reduction processes, with little electrochemical evidence for ground state interactions between the rhenium centres mediated by the tricopper cluster [58].

## Main group cluster bridges

Diethynyl carboranes have recently attracted attention as possible conduits for electronic effects, and the mechanism through which these effects are transmitted through the cage has been a source of some interest [59]. Electrochemical studies of $\{Co_2(CO)_4(dppm)\}_2(\mu\text{-}Me_3SiC_2\text{-}1,12\text{-}CB_{10}H_{10}CC_2SiMe_3)$ using both cyclic and differential pulse voltammetric methods revealed two sequential oxidation processes and two sequential reduction processes separated by 105 mV and 80 mV, respectively [60]. While these redox processes were qualitatively similar to those of an analogous $1,4\text{-}C_6H_4$ bridged species [61], DFT analysis of the radical cations revealed a different underlying electronic structure in each case. The SOMO of the aryl-bridged species featured considerable aryl π-character, while the SOMO of the carborane spaced species was essentially localised on the $Co_2C_2$ clusters. It was concluded that the carborane cluster cage acts as a more or less σ-bridge [62].

A complimentary study by Hawthorne's group using $Fe(CO)_2Cp$ based redox probes revealed a diminished interaction through the diethynyl carborane moiety when compared with $\{Fe(CO)_2Cp\}_2(\mu CB_nH_nC)$ ($n = 8$, 10). Interpolation of a mercury centre between two cages also resulted in the observation of a single irreversible oxidation wave by CV [63].

**Structure 4**

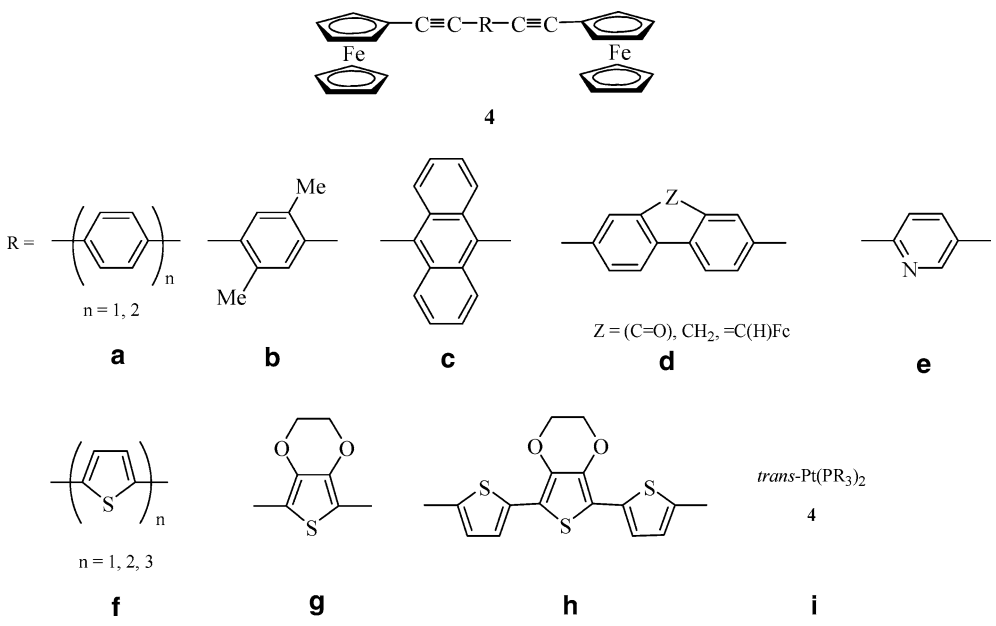


## Diethynyl aromatic bridges

In the case of ferrocene redox probes, introduction of aromatic moieties within the carbon chain (**4**) results in the observation of an apparently single, quasi-reversible oxidation process, albeit with a relatively large peak–peak separation in several cases. While the broadness of the wave probably indicates the presence of two closely spaced processes, it is clear that these bridges are not well-suited to the task of promoting interactions between the remote ferrocene moieties. The oxidation potentials of these complexes are sensitive to the inductively electron withdrawing (phenyl) or donating (thiophenyl) nature of the ethynyl-based bridges [35, 64–69].

In the case of the 2,5-diethynylpyridine bridged system **4e** the ferrocenyl centres are formally non-degenerate, but only a single oxidation process was observed with $\Delta E_p$ (64 mV) consistent with essentially independent, and identical, redox behaviour at these sites. However, methylation of the pyridine nitrogen centre in **4e** results in a significant splitting of the oxidation events ($\Delta E = 161$ mV) when the non-coordinating electrolyte $[NBu_4][B(C_6F_5)_4]$ is employed in $CH_2Cl_2$. This switching in behaviour and localisation of charge on the distinct ferrocenyl termini has been suggested as the basis for a single molecule transistor which would pass charge by electron hopping, not through-bond coupling of the redox sites [70].

Not unexpectedly, the magnitude of the redox wave separation $\Delta E$ is sensitive to the regiochemistry of the substitution around the aromatic ring. For example, both 1,8- (**5a**) and 1,5- (**5b**) bis(ferrocenylethynyl)naphthalene derivatives both display two chemically reversible diffusion-controlled one-electron oxidation couples arising from the ferrocenyl moieties, with $\Delta E$ significantly larger in the case of **5a** (109 mV) than **5b** (60 mV), due to an unresolved combination of through-bond and through-space factors [33].

However, incorporation of the redox active probe group directly into the ligand π-system results in far greater interactions between the remote sites. While there are numerous examples of the preparation and characterisation of metal complexes, and related polymers, featuring the $ML_x–C \equiv CArC \equiv C–ML_x$ motif, surprisingly few of these studies have also incorporated electrochemical methods, and even fewer have explicitly addressed the nature of the mixed-valence compounds which may be derived from them.

**Structure 5**

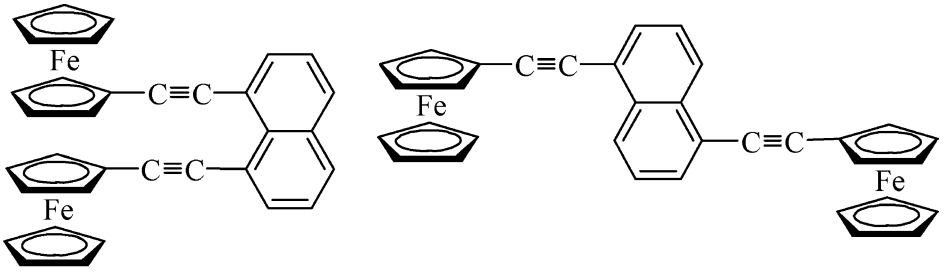

In early work, the complexes [*trans*-{FeCl(dmpe)$_2$}$_2$(μ-1,4-C ≡ $CC_6H_4$C ≡ C)], bearing the strongly electron-donating dimethylphosphinoethane ligands, were prepared and found to undergo two sequential, one electron oxidation processes, separated by ca. 0.2 V ($K_c = 2.4\times10^3$) in $CH_2Cl_2$ containing 0.2 M [$NBu_4$][$ClO_4$] (CARE!), and as a result the mono-cation was assumed to be a Class II mixed valence species. An irreversible, apparently two electron anodic process was also observed at higher potentials. The diffusion-controlled behaviour of the first two oxidation events was taken as an indication of limited structural rearrangement accompanying the redox steps. Both the mono and dications were found to be ESR active, but only broad unresolved lines were obtained at low temperatures [71].

Since this initial investigation, the electrochemical response of several related pseudo-octahedral [{$ML_x$}$_2$(μ-1,4-C ≡ $CC_6H_4$C ≡ C)] complexes have also been reported [72–76]. The nature of the metal end-capping group plays a significant role in determining the magnitude of coupling in these systems, and in the case of {Pt($C_6H_3CH_2NMe_{22}$-2,6}$_2$(μ-1,4-C ≡ $CC_6H_4$C ≡ C) (**6**) [77] and the *bis*-bimetallic complex [{$Ru_2$(ap)$_4$}$_2$(μ-1,4-C ≡ $CC_6H_4$C ≡ C)] (ap = 2-anilinopyridinate) [78] CV measurements indicated independent redox behaviour associated with the metal sites. For example, in the case of the platinum species **6**, only a single, irreversible oxidation wave was observed by cyclic voltammetry corresponding to the removal of a total of four electrons in two overlapping (or simultaneous) Pt(II/IV) oxidation steps.

The compound {Fe(dppe)Cp*}$_2$(μ-C ≡ $CC_6H_4$C ≡ C) (**7a**) displays a reversible electrochemical response, the cyclic voltammogram of this compound being characterised by two one-electron waves with a current ratio of unity. The large separation of the half-wave potentials $\Delta E = 0.26$ V indicates the thermodynamic stability of the mixed-valence form with respect to disproportionation ($K_c = 2.6\times10^4$), which whilst smaller than the value associated with the first two oxidation waves in the "all-carbon" bridged species {Fe(dppe)Cp*}$_2$(μ-C ≡ CC ≡ C) ($\Delta E = 0.71$ V, $K_c = 1\times10^{12}$) [79], is sufficiently large to allow synthetic preparation of **[7a]**$^+$ and **[7a]**$^{2+}$ free of contamination and isolation as the $PF_6^-$ salts [74]. Magnetic susceptibility measurements of the dicationic species **[7a]**$^{2+}$ are consistent with antiferromagnetic coupling of the (formally) 17-electron metal centres, and in agreement with the ESR spectrum of this material, which exhibits three broad *g* tensor components without the characteristic hyperfine coupling that might be expected of metal centred radicals. When taken together with the decreased ν(CC) frequency, these data support a description of **[7a]**$^{2+}$ which involves an appreciable contribution from the cumulated canonical form. The behaviour of the mixed-valence form **[7a]**$^+$ is complicated by an apparently conformationally based distinction between valence-trapped and detrapped forms of the compound. Thus the Mössbauer spectrum of **[7a]**$^+$ contained three sets of doublets characteristic of Fe(II), Fe(III) and an intermediate valence state indicative of the de-trapped state. The relative proportions of the doublets varied from batch to batch of solid, but each spectrum was temperature independent between 77 and 280 K. At lower temperatures (5 K) an increase in the amount of Fe(II) character relative to that of the de-trapped state was observed, and attributed to stabilisation of a bridge-localised radical. Infrared spectroscopy in both solid and solution state did not discredit this suggestion, and while the precise mechanism is perhaps unclear, it does appear certain that the 1,4-diethynylbenzene ligand is capable of delocalising an unpaired electron between the two iron centres, which are separated by almost 12 Å [74].

The influence of the bridging aromatic moiety has also been considered through electrochemical measurements of closely related series of complexes featuring a common metal–ligand combination and a range of diethynyl aromatic bridging moieties. Direct comparison of the electrochemical response of {Fe(dppe)Cp*}$_2$(μ-C ≡ C–X–C ≡ C) species (X = C ≡ CC ≡ C, 2,5-thiophene) revealed a greater separation of the Fe(II/III) oxidation processes in the case of the polyethyndiyl ligand (0.43 V vs. 0.34 V), although analysis of the NIR transitions suggest little difference in the coupling parameter $V_{ab}$ [80]. Substitution of the fully conjugated ligands by alkyndiyl bridges incorporating methylene groups lead to weakly coupled mixed-valence materials, in which optically induced electron transfer appears to involve two different pathways arising from transitions between the HOMO-1 → SOMO and HOMO-n → SOMO [81].

It has been shown through a combination of electrochemical and spectroscopic techniques and semi-empirical calculations that coupling between two *trans*-MCl(dppm)$_2$ fragments (M = Fe, Ru, Os) through diethynylaromatic ligands C ≡ CArC ≡ C follows the order Ar = 2,5-$C_4H_2S$ > 1,4-$C_6H_4$ > 2,5-$C_5H_3N$ > 1,3-$C_6H_4$, a result which was attributed to the relative energy change associated with the adoption of a quinoidal structure [73, 75]. The ruthenium fragments were

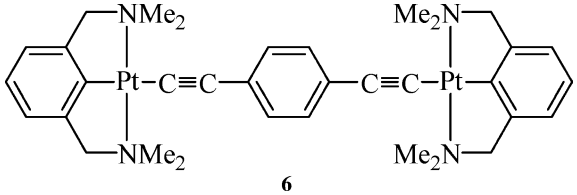


**6**

**Structure 6**

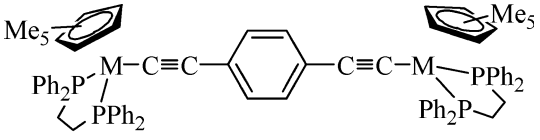


**M = Fe (7a), Ru (7b)**

**Structure 7**

more strongly coupled than the analogous Fe or Os species, a trait attributed to the better interactions between the π-donating ligand and the metal centre [82].

Recent work from this group has been concerned with bimetallic complexes derived from 1,4-diethynylbenzene, 1,4-diethynylnaphthalene, and 9,10-diethynylanthracene [83]. The cyclic voltammetric response of each compound in the series **7b**, **8**, and **9** was similar, being characterised by two reversible oxidation processes separated by ca. 300 mV. The thermodynamic stability of the mono-oxidised forms with respect to disproportionation was matched by the kinetic stability of each member of the series and chemical oxidation ($AgPF_6$) allowed isolation of $\mathbf{[7b]}^{n+}$, $\mathbf{[8]}^{n+}$ and $\mathbf{[9]}^{n+}$ ($n = 1$, 2) as the $PF_6^-$ salts in essentially quantitative yield. Upon oxidation of the 36-electron compounds to the corresponding 35-electron (mono-oxidised) and 34-electron (di-oxidised) species the ν(CC) band of the ligand was found to shift to progressively lower energy, consistent with the evolution of a more cumulated electronic structure. This interpretation is fully consistent with DFT models of $\mathbf{[7b]}^{n+}$, which indicate a substantial delocalisation of the frontier orbital over the metal centre and the diethynyl benzene ligand [84].

The UV-Vis spectra of the mono-oxidised species were characterised by relatively intense MLCT bands, together with a set of vibrationally structured bands at lower energy, centred between 19,000 and 12,000 $cm^{-1}$, with profiles very similar to those of the appropriate aryl radical cation. This observation, together with the IR data, suggests the bridge orbitals are significantly involved in the redox process. In addition, each species $\mathbf{[7b]}^{+}$, $\mathbf{[8]}^{+}$ and $\mathbf{[9]}^{+}$ exhibited an overlapping series of absorptions in the NIR region with remarkably similar profiles and energies, with the lowest energy band maximum near 5,000 $cm^{-1}$ in each case. The similar electrochemical, vibrational and electronic signature of these monocations suggests little variation in the magnitude of electronic coupling through these ligands.

Further oxidation to the diamagnetic dicationic species, $\mathbf{[7b]}^{2+}$, $\mathbf{[8]}^{2+}$ and $\mathbf{[9]}^{2+}$ resulted in the collapse of the NIR and vibrationally structured visible bands associated with the mixed valence species. The electronic structure of the dications were characterised by one or two bands in the visible region, which are probably MLCT/LMCT in nature [83].

Regardless of the nature of the metal fragment employed, *meta*-substitution patterns lead to less strongly electronically coupled systems. For example, for 1,3,5-

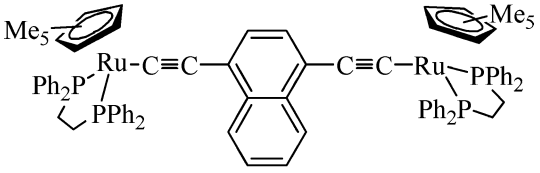


**8**

**Structure 8**

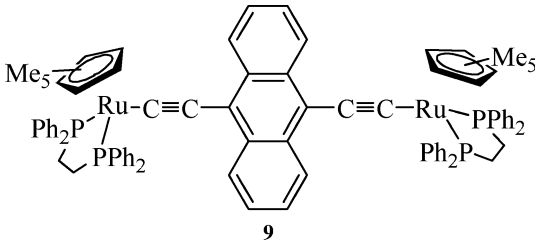


**9**

**Structure 9**

*tris*(ferrocenylethynyl)benzene in which the ferrocenyl moieties are arranged in mutually *meta* positions around the aromatic ring only a single anodic process was detected by cyclic voltammetry [85, 35]. The wave has the shape of a one-electron process, but was shown by controlled potential coulometry to consume three electrons per molecule. This is indicative of three independent, one-electron processes arising from the independence of the ferrocenyl centres [86]. No low energy absorption bands were observed.

As with 1,4-disubstituted systems, incorporation of the metal centre directly into the conjugated ligand framework can result in more significant interactions with $\Delta E$ values of up to 180 mV being observed in the case of complexes such as **10, 11** and **12** [78, 87–89]. The magnetic properties [90, 91] and NLO response [92, 93] of these weakly interacting systems which can have high spin configurations associated with their higher oxidised states may be a source of interest for future investigations.

For example, the mixed-valence cation $\mathbf{[11]}^{+}$ exhibits two ν(C ≡ C) bands corresponding at an approximate level to vibrations associated with Fe(II)–C ≡ C and Fe(III)–C ≡ C moieties, indicating electron transfer between the sites to be slow on the IR timescale, although DFT analysis suggests an appreciable amount (22.9%) of the unpaired spin density resides on the aromatic portion of the bridging ligand. Mössbauer spectroscopy also indicates the presence of distinct Fe(II) and Fe(III) centres [90]. Weak, solvent independent bands ($\epsilon_{max}$ ca. 500 $M^{-1}$ $cm^{-1}$) were found in the NIR region under the tail of the LMCT bands. By

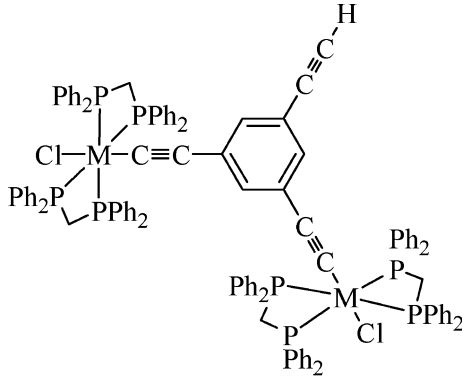


**10 (M = Ru, Os)**

**Structure 10**

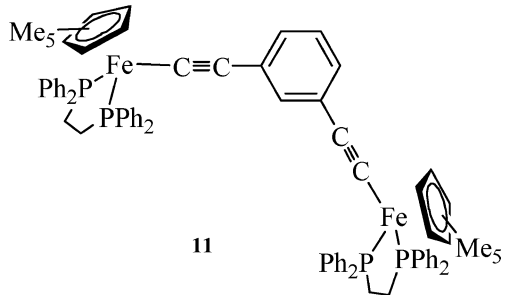


11

**Structure 11**

assuming Gaussian line shapes it was possible to deconvolute the absorption into two bands, one assigned to a ligand–field (LF) transition associated with the Fe(III)(dppe)Cp* fragment, the other to the Fe(II)–Fe(III) IVCT transition. The Gaussian line-fit of the IVCT band was found to have half-height bandwidth close to that predicted by Eq. 3. Using Eq. 4, and assuming the Fe...Fe separation to be a reasonable estimate of the electron transfer distance, gave a value of $V_{ab}$ of 0.020 eV (160 $cm^{-1}$) [90].

The paramagnetic species **[11]**$^{2+}$ contains two low spin Fe(III) centres, with magnetic susceptibility measurements and DFT calculations indicating a triplet ground state, with a singlet–triplet energy gap $\Delta E_{TS} = 2J = 130.5 \pm 0.2$ $cm^{-1}$. While this value is not as large as found in organic radicals bridged by *meta*-phenylene spacers, the magnitude of the ferromagnetic coupling observed in this system is interesting, given the $>10$ Å (1 nm) separation of the iron centres [91].

In the case of the trinuclear species **[12]**$^{+}$ the interpretation of the mixed-valence behaviour must take into account the electron transfer between three sites, and a modified form of Eq. 4 is employed, as given in Eq. 10 [94].

$$V_{ab} = 2.06 \times 10^{-2} \frac{\sqrt{\bar{\nu}_{max} \varepsilon_{max} \bar{\nu}_{1/2}}}{r\sqrt{2}}. \quad (10)$$

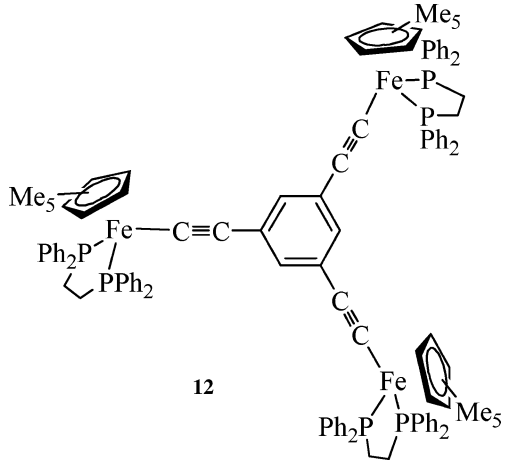


12

**Structure 12**

Within the limits of the various assumptions made, the coupling in **[12]**$^{+}$ was the same as that in **[11]**$^{+}$.

The NIR spectrum of the diradical **[12]**$^{2+}$ contained three bands, one of which was assigned to the LF transitions associated with the formally Fe(III) centre, and two attributed to IVCT type processes [90]. The two IVCT processes probably originate from the magnetic interactions between the two $S = 1/2$ centres. According to ESR and magnetic data, at 20 °C both singlet and triplet states are populated and different electron transfer pathways are expected to occur between the singlet and triplet states. However, it was not possible on the basis of the data to hand to assign the IVCT bands to the singlet or triplet states, and a full determination of the thermodynamic parameters, which relies on an estimate of both $\nu_{max}$ and $\epsilon$ could not be performed [90].

The trimetallic trication **[12]**$^{3+}$ displayed temperature dependent magnetic susceptibility consistent with the thermal population of excited doublet ($S = 1/2$) lying above the quartet ($S = 3/2$) ground state by some $18.7 \pm 0.5$ and $28.8 \pm 0.5$ $cm^{-1}$, and DFT level calculations confirm the stability of the high-spin ground state [91].

It is clear that the extent of electronic and magnetic coupling in ethynyl-aromatic bridged polymetallic complexes is dependent on a combination of features relating to both the metal and the bridge [72]. If the molecular design rules which influence these parameters are to be generalised, considerably more investigations of a wider range of complexes will be necessary.

## Metal bis(acetylide) bridges

Various efforts have been made to include metal centres within the bridging moiety [10, 66, 67, 72, 95]. The introduction of a diethynyl-platinum motif as the spacer, as in **13**, or within a more complicated architecture, as in **14**, does not promote any electrochemically detectable interactions between the remote ferrocene moieties. Similarly, in the case of [{*trans*-RuCl(dppe)$_2$}(μ-C ≡ CPt(PBu$_3$)$_2$C ≡ C)], only a single, apparently two electron oxidation process was observed for the $Ru^{II/III}$ couples [72]. However, the question of to what extent the Pt(II) centre promotes or disrupts π-conjugation along an ethynyl-based chain remains an open question, and the very recent work of S.R. Marder et al. using organic redox probes suggests that it may be possible to engineer modestly delocalised systems based on the *trans*-C ≡ C–$Pt^{II}$–C ≡ C fragment [96]. It should also be noted that several related studies have suggested this motif may be

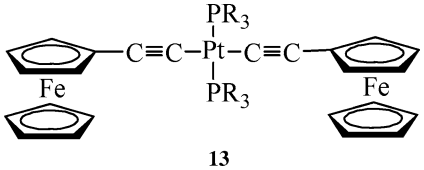


13

**Structure 13**

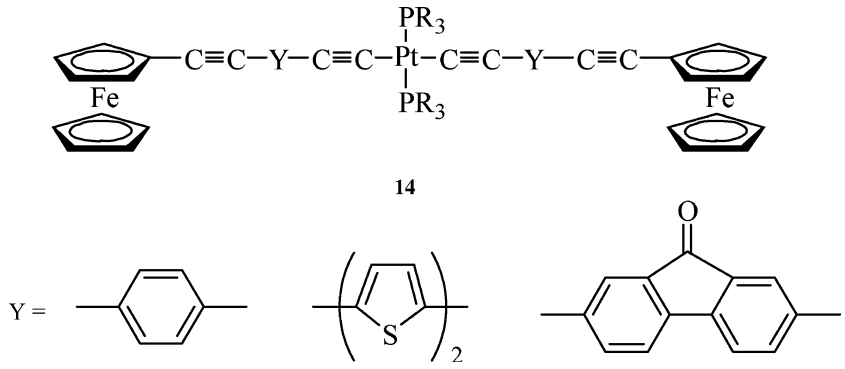


**Structure 14**

more suitable for allowing interactions in photoexcited states [97–101]. The introduction of a mercury centre also served to sever electrochemically detectable interactions between Ru(dppe)Cp* fragments along a polycarbon chain, a result attributed to the lack of a Hg contribution in the HOMO [102].

More pronounced interactions in the ground state are mediated by octahedral metal centres, most thoroughly represented by the family of complexes *trans*-M(C ≡ CFc)$_2$(L$_4$). In the case of the complexes *trans*-Ru(C ≡ CFc)$_2$(dppx)$_2$ (**15**) (dppx = dppm (**15a**) [103–105]; dppe (**15b**) [106]) three chemically reversible oxidation processes are revealed by cyclic voltammetry. Similar results have been found for a related manganese system [107]. By comparison with the oxidation potentials of model materials these processes were assigned to the sequential oxidation of the ferrocene moieties ($\Delta E$ ca. 200 mV), and the ruthenium II/III couple. Extension of the carbon bridge from (C ≡ C) to (C ≡ CC ≡ C) has the expected result of diminishing the separation of the ferrocene-based oxidation events ($\Delta E$ = 139 mV) [106], but still supports the unusual observation that the metallocarbon backbone is more effective than the pure carbon bridge at promoting electronic interactions in the ferrocene series, despite the increase in Fe...Fe separation.

The mono- and dications *trans*-[Ru(C ≡ CFc)$_2$(dppm)$_2$]$^+$ (**[15a]$^+$**) and *trans*-[Ru(C ≡ CFc)$_2$(dppm)$_2$]$^{2+}$ (**[15a]$^{2+}$**) each exhibit at least two bands in the NIR region, which are not present in the neutral complex. In both cases the lower energy transition, the position of which is solvent independent, is assigned to localised d–d transition associated with Fe(III), while

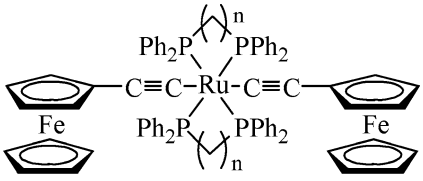


**n = 1 (15a), 2 (15b)**

**Structure 15**

the higher energy band is assigned to the Ru(II) → Fe(III) electron transfer processes [104]. While for the dication, a simple two-state model [Scheme 3, diagram (a)] suffices to explain the origin of the NIR transition, a three-state potential energy diagram has been proposed to rationalise the electronic structure of the monocation (Scheme 3). In the dicationic species each iron centre is in the Fe(III) state, and hence electron transfer between them is not possible. In the scheme, $h\nu$ is the energy required to move from the thermodynamically stable ground state configuration (A) to state B, and includes the reorganisation energies and $\Delta G^o$ terms.

In the case of the monocations, the three state potential energy diagram [Scheme 3, diagram (b)] provides a better description. In Wolf's analysis, the three possible electronic configurations ($Fe^{III}$–$Ru^{II}$–$Fe^{II}$, $Fe^{II}$–$Ru^{III}$–$Fe^{II}$, $Fe^{II}$–$Ru^{II}$–$Fe^{III}$) were termed C, D and E for ease of reference. The photon h$\nu$' provides energy necessary to move an electron from state C, which is isoenergetic with E, to D. State D can collapse to either C or E, and therefore photoexcitation of state C by h$\nu$' provides a mechanism for charge transfer across the ruthenium bis(acetylide) bridge. When compared with the simple species **1**, the role of the Ru centre is to lower the activation barrier, $\Delta G^*_{th}$, to electron transfer. This suggestion is in complete agreement with the trends observed in the series of compounds **16**, for which the interaction between the two ferrocene moieties (as measured by $\Delta E$) and energy of the lowest energy NIR band decreases as the oxidation potential of the Ru centre is increased. This general picture is reinforced by studies of the closely related complexes [Ru(C ≡ CMc)(L$_2$)Cp']$^{n+}$ (Mc = Fc, Rc; L = PPh$_3$, dppe; Cp' = Cp, Cp*, n = 0, 1). While electrochemical studies indicated a number of oxidation processes, Mössbauer spectroscopy was used to confirm oxidation of the iron centre in the mono-oxidised derivatives, and allowed assignment of one of the two observed NIR bands to a $Ru^{II} \rightarrow Fe^{III}$ transition [108, 109]. The chemically irreversible nature of the oxidation events associated with Ru(C ≡ CC ≡ CFc)(dppx)Cp (dppx = dppm, dppe) precluded a detailed analysis of the oxidised derivatives of this complex [110].

**Scheme 3**

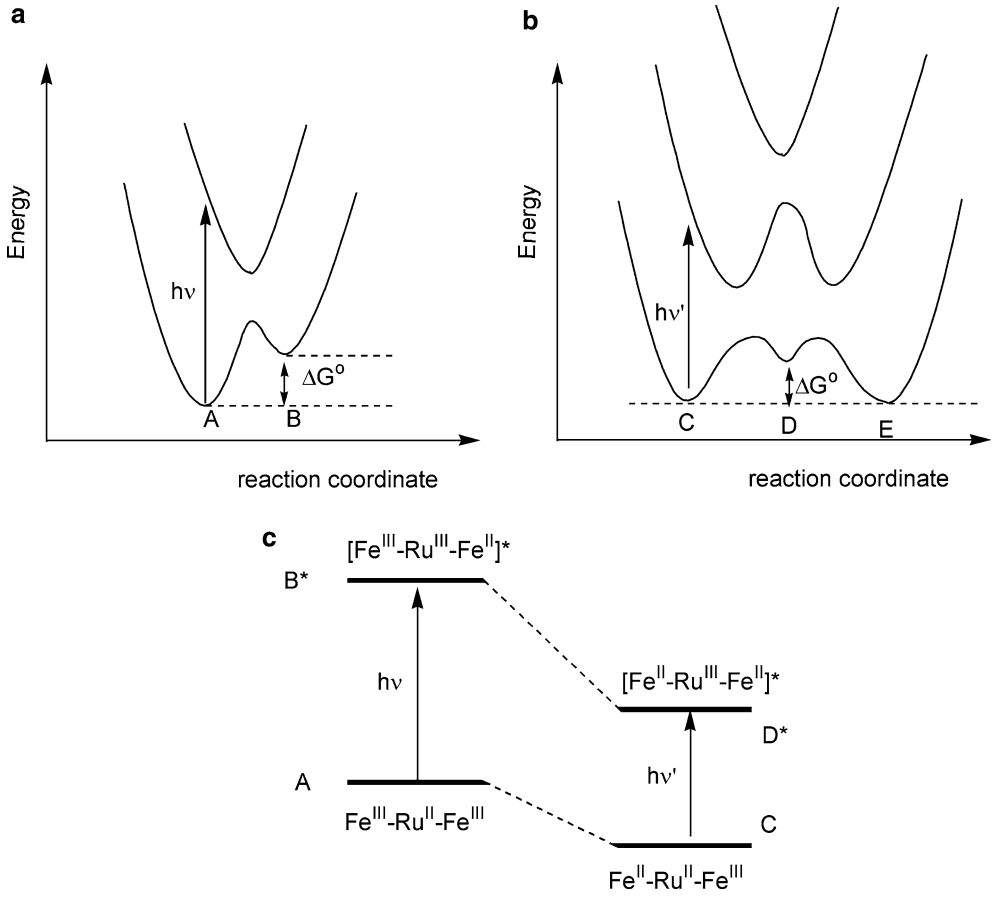


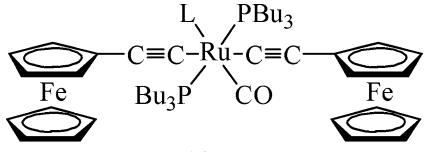


**16**

L = CO, $NC_5H_5$, $P(OMe)_3$

**Structure 16**

More elaborate, multimetallic bridges have been investigated as potential conduits of electronic effects in recent times, generally featuring ferrocenyl probe groups [111–114]. The diplatinum bridged species $[Pt_2(dppm)_2(C \equiv CFc)_2]$ has been used to demonstrate interactions between the remote ferrocenyl moieties through the Pt–Pt bond [115]. The CV of $[Pt_2(dppm)_2(C \equiv CFc)_2]$ displays two quasi-reversible one-electron oxidation waves associated with the Fc moieties separated by ca. $267 \pm 10$ mV, suggesting considerable interactions between them mediated by the Pt–Pt single bond. In situ generation of $[Pt_2(dppm)_2(C \equiv CFc)_2]^+$ by oxidation with excess ferrocinium cation revealed a NIR transition at $\bar{\nu}_{max} = 11300 \pm 50\,cm^{-1}$ ($\epsilon = 610 \pm 10\,M^{-1}\,cm^{-1}$), $\Delta\bar{\nu}_{1/2} = 2800\,cm^{-1}$. This is somewhat lower in energy than the $Ru^{II} \rightarrow Fe^{III}$ transition observed by Wolf and colleagues in their $Ru(dppm)_2$ spaced analogues, and is therefore not consistent with assignment as a $Pt^{I} \rightarrow Fe^{III}$ transition. In the $Pt_2$-bridged case the band is assigned to a direct $Fe^{II} \rightarrow Fe^{III}$ transition. Assuming $r = 14.474(2)$ Å (the crystallographically determined Fe...Fe distance), the Hush relationships allow estimation of $V_{ab} = 190 \pm 20\,cm^{-1}$ from the spectroscopic data. On the basis of energy considerations, it is concluded that the primary mechanism of interaction arises from inductive and/or magnetic interactions through the π-orbitals of the bridging moiety rather than delocalisation effects. Addition of an AuX (X = Cl, Br) fragment to the Pt–Pt bond gives A-frame complexes which display negligible interactions between the ferrocenyl centres [115].

The diruthenium(III) tetra(amidinate)-bridged complexes **17a-c** give rise to essentially identical DPVs with three one-electron oxidation processes observed between 0.4 and 1.0 V, together with an $Ru_2$ centred reduction. The more soluble alkoxy substituted derivatives were amenable to spectroelectrochemical analysis, with $\mathbf{[17c]^+}$ giving rise to a broad, low energy band which tailed from the NIR into the IR region (band 1). Further oxidation to $\mathbf{[17c]^{2+}}$ gave an additional band at $\lambda_{max} = 6{,}040\,cm^{-1}$ (band 2). The oxidation processes were assigned to sequential oxidation of the $Ru_2$ core and the Fc moieties, with band 1 assigned to $Fe^{II} \rightarrow Ru_2^{III,IV}$ charge transfer and band 2 to $Fe^{II} \rightarrow Fc^{III}$ charge transfer across the

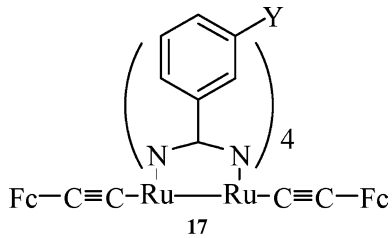


**17**

Y = H (**a**), OMe (**b**), OBu (**c**)

**Structure 17**

metallocarbon bridge. Preliminary analysis of band 2 suggests $\mathbf{[17]}^{2+}$ is a fully delocalised system, with the $V_{ab}$ term for $Fe^{II} \rightarrow Fe^{III}$ charge transfer ca. 3,000 $cm^{-1}$ [113].

Diethynyl di- and triferrocenyls have also been considered as potential bridging moieties, and interactions between remote ferrocenyl or $Co_2C_2(CO)_4$(dppm) redox probes through the $Fc_n$ core in complexes **18a-d** investigated [116]. While detailed orbital analysis was not available, electrochemical studies provide a series of interesting observations, including: the interpolation of the $Fc_2$ unit does not impede electronic interactions between the remote groups, although more attenuation is apparent with the $Fc_3$ moiety; the terminal groups and the oligoferrocene core act almost independently.

In contrast, the extended metal atom chain (EMAC) complex **19**, which is formally comprised of a diamagnetic singly bonded $[Co_2]^{4+}$ and an isolated $Co^{2+}$ centre, is not as effective a conduit of electronic effects between the Fc moieties. Cyclic and differential pulse voltammetry revealed three chemically reversible oxidation processes, the second being likely comprised of two overlapping and unresolved events and tentatively assigned to the sequential oxidation of the ferrocene moieties. On the basis of the width of the unresolved peak in the DP trace, a value of $\Delta E = 71$ mV was estimated [117, 118]. Unfortunately, attempts to observe the oxidised products were hampered by decomposition of the products during preparative electrochemical or chemical oxidation of **19** [119, 120].

A number of complexes featuring bis(ferrocenylethynyl) in a *cis* geometry have also been reported [121–123]. While these species can be used as redox-active "molecular tweezers", the interest from the present perspective lies in the reductive coupling of the acetylide ligands which occurs following oxidation of the

**Structure 18**

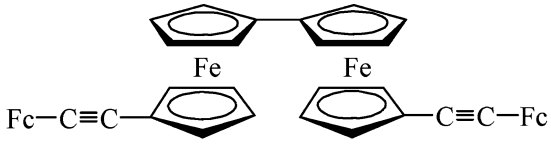


**18a**

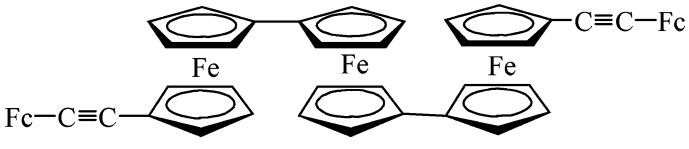


**18b**

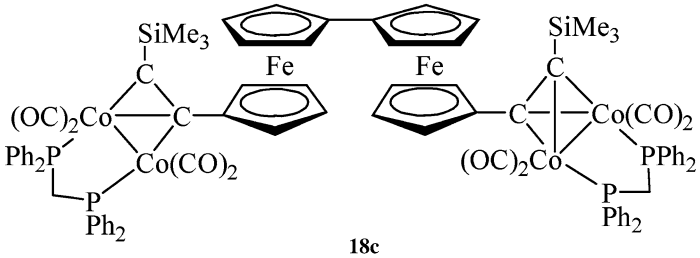


**18c**

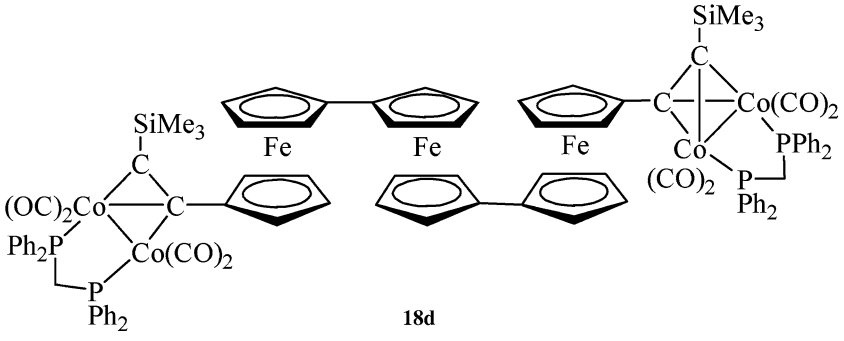


**18d**

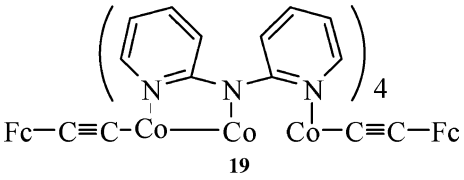

**19**

**Structure 19**

ferrocenyl termini either chemically or electrochemically in titanium derivatives (Scheme 4).

## Heterometallic species

The task of evaluating interactions between different metal centres through ethynyl-based bridging ligands using electrochemical methods can be complicated by differing interpretations of the observed electrochemical response of the system in terms of either metal centred redox events (i.e simple donor–acceptor systems), or redox processes which involve more extensively delocalised orbitals. Solvation effects can also alter $E^0$ values, and it is important to bear in mind that direct comparisons of electrode potentials of bimetallic complexes with those of model compounds is only valid if the relative solvation energies of the compounds are in their various oxidation states do not differ significantly [124, 125].

In general, mixed-metal systems are weakly to moderately coupled, and can often be treated in terms of metal centred oxidation events and electronic transitions between distinct metal based chromophores. Compounds of this type are therefore well described by a modified form of the Hush theory outlined in the introduction. For a prototypical $M^{II}_A$-bridge-$M^{III}_B$ with metal $M_A$ and $M_B$ assigned arbitrary oxidation states of +2 and +3, respectively, the energy of the MMCT band $E_{op}$ (in $cm^{-1}$) can be expressed in terms of the free energy difference $\Delta G^o$ between the redox isomers $M^{II}{}_A$-bridge-$M^{III}{}_B$ and $M^{III}{}_A$-bridge-$M^{II}{}_B$ and the combined inner and outer sphere reorganisation energies, $\lambda$ (Eq. 11).

$$E_{op} = \Delta G^{\circ} + \lambda. \tag{11}$$

If solvation factors are ignored, the free energy difference $\Delta G^o$ can be approximated by the difference in electrode potentials associated with each metal site through

$$\Delta G^{\circ} = \frac{\Delta E^{\circ} F}{11.97} \tag{12}$$

but such an approximation becomes less valid as hydrogen bonding between the metal/ligand fragment and the solvent become important [124].

In complexes such as *trans*-Pt(Ph)(C ≡ CML$_n$)(PEt$_3$)$_2$ (**20**, **21**) the electrochemical response of the complex can be interpreted in terms of the ML$_n$C ≡ CR fragment featuring a relatively strong, but electrochemically "innocent", platinum donor group [126]. The mixed iron/rhenium complex [{Cp*(dppe)-Fe}(μ-C ≡ CC$_6$H$_4$C ≡ C){Re(CO)$_3$(bpy)}] exhibits a quasi-reversible reduction process which is only 0.02 V less favourable than the bpy centred reduction in Re(C ≡ CC$_6$H$_4$C ≡ CH)(CO)$_3$(bpy), and an iron centred oxidation some 0.04 V more favourable than the oxidation of Fe(C ≡ CPh)(dppe)Cp*, indicating a simple relationship in which both metal centres act as moderately electron donating substituent. In agreement with this interpretation DFT analysis of the electronic structure of the H-substituted model material [{Cp(dHpe)Fe}(μ-C ≡ CC$_6$H$_4$C ≡ C)Re(CO)$_3$(bpy)] reveals a predominantly bpy-centred LUMO and an iron-centred HOMO [127].

In [{RuCl(dppm)$_2$}(μ-C ≡ CC$_6$H$_4$C ≡ C){OsCl(dppm)$_2$Cl}], two oxidation processes are observed by CV, which were assigned to the sequential oxidation of the Os and Ru fragments, but both of which are at less positive potentials than model mononuclear complexes *trans*-{MCl(C ≡ CC$_4$H$_4$C ≡ CH)(dppm)$_2$} (M = Ru, Os) [126]. Such behaviour might be rationalised either by assuming that the oxidised osmium fragment is a better donor than the ethynyl moiety, or that the electronic structure of [{RuCl(dppm)$_2$}(μ-C ≡ CC$_6$H$_4$C ≡ C){OsCl(dppm)$_2$Cl}]$^+$ is not well described in terms of isolated Ru(II) and Os(III) fragments. Similarly, the redox response of the diynyl bridged species {Cp*(dppe)Fe}(μ-C ≡ CC ≡ C){Re(PPh$_3$)(CO)Cp*} [128] is characterised by two anodic processes assigned to sequential oxidation of the Fe and Re fragments, which

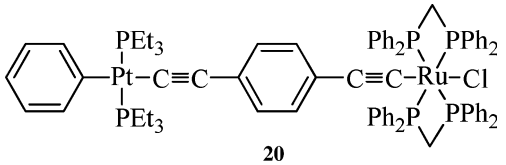

**20**

**Structure 20**

**Scheme 4**

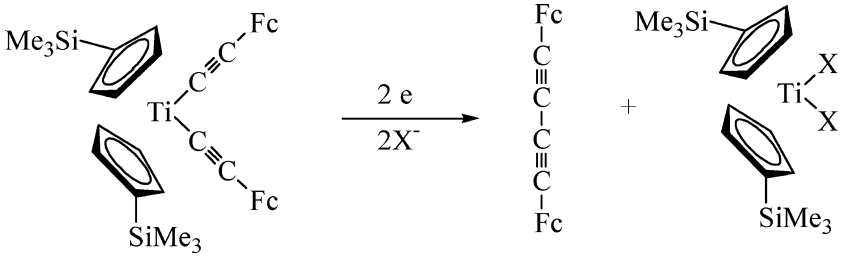

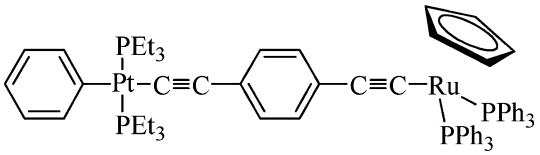

21

**Structure 21**

occur at potentials less thermodynamically favourable than the corresponding oxidation of model mononuclear species. When the electrochemical result is coupled with a detailed spectroscopic and DFT investigation [129], the best resonance description which can be attributed to the monooxidised form would be derived from a predominantly iron centred oxidation. The NIR band observed in $[\{Cp^*(dppe)Fe\}(\mu\text{-}C \equiv CC \equiv C)\{Re(PPh_3)(CO)Cp^*\}]^+$ is therefore attributed to a photoinduced $Re^{II} \rightarrow Fe^{III}$ transition, and Hush style analysis of the band shape gives $V_{ab} = 0.019$ eV.

A combination of CV and electronic structure calculations using DFT, ZINDO and ELF methods has been used to probe the interactions which occur between the metal end-caps in $Co_2[\mu\text{-}\eta^2\text{–}Me_3SiC \equiv CC_2C \equiv C\{Ru(PPh_3)_2Cp\}](CO)_4(dppm)$ and $Co_2[\mu\text{-}\eta^2\text{–}Me_3SiC_2C \equiv CC \equiv C\{Ru(PPh_3)_2Cp\}](CO)_4(dppm)$ [130]. In this case, CV revealed two facile oxidation events, both of which occur at much less positive potentials than the $[Co_2C_2]^{0/+}$ couple in the corresponding model $Co_2(\mu\text{-}\eta^2\text{–}Me_3SiC \equiv CC_2C \equiv CSiMe_3)(CO)_4(dppm)$ or $Co_2(\mu\text{-}\eta^2\text{–}Me_3SiC_2C \equiv CC \equiv CSiMe_3)(CO)_4(dppm)$ and also at a less positive potential than the Ru(II/III) couple in $Ru(C \equiv CPh)(PPh_3)_2Cp$. Electronic structure calculations revealed extensively mixed $Co_2C_2/C_n/Ru$ character in the HOMO, and consequently the electrochemical events cannot be considered in terms of the properties of isolated redox active fragments.

Recently, a simple synthesis of metal complexes containing the cyanoacetylide ligand has been developed [131]. The ready availability of compounds such as $Ru(C \equiv CC \equiv N)(PPh_3)_2Cp$ and $Fe(C \equiv CC \equiv N)$(dppe)Cp by this method allows access to the isomeric hetero bimetallic species $Ru\{C \equiv CC \equiv N[Fe(dppe)Cp]\}(PPh_3)_2Cp$ (**22**) and $Fe[C \equiv CC \equiv N\{Ru(PPh_3)_2Cp\}](dppe)Cp$ (**23**). The electrochemical response of each compound is characterised by two oxidation events at 0.62 and 1.22 V (**22**) and 0.66 and 1.37 V (**23**), which may be compared with the oxidation potentials of $Ru(C \equiv CC \equiv N)(PPh_3)_2Cp$ (0.92 V), $Fe(C \equiv CC \equiv N)$(dppe)Cp (0.53 V) and the nitrile species $[Ru(NCPh)(PPh_3)_2Cp]PF_6$ (1.30 V) and $[Fe(NCPh)(dppe)Cp]PF_6$ (0.83 V) measured under identical conditions [0.1 M $NBu_4BF_4$ in $CH_2Cl_2$, all Pt electrodes, potentials quoted vsersus internal $Fc/Fc^+$ (0.46 V vs. SCE) or $Fc^*/Fc^{*+}$ (−0.02 V vs. SCE)]. Infra-red spectroelectrochemical investigation of the monocations reveals a significant decrease in the energy of the $\nu(C \equiv CC \equiv N)$ vibrational bands, consistent with a contribution from the ligand to the redox active orbital. Relatively intense NIR bands are also found ($[\mathbf{22}^+]$ $\nu_{max} = 9{,}600$ cm$^{-1}$, $\epsilon = 5{,}600$ M$^{-1}$ cm$^{-1}$; $[\mathbf{23}^+]\nu_{max} = 9{,}200$ cm$^{-1}$, $\epsilon = 2{,}500$ M$^{-1}$ cm$^{-1}$), although in the absence of confirmation of the extent of localisation/delocalisation of the unpaired electron in these complexes, it is difficult to conclusively assign these transitions to MMCT processes [132].

However, if several critical assumptions are made, it is possible to draw out some intriguing aspects for future investigation. Given the structural similarities of the iron centres in complexes such as $\mathbf{[11]}^+$ [90] and related iron acetylides [133] and the relatively limited solvent dependence of the redox response of closely related half-sandwich complexes such as $Ru(CN)(PPh_3)_2Cp$ [134] it seems reasonable to assume that the solvation energy associated with the $Ru(PPh_3)_2Cp$ and Fe(dppe)Cp fragments changes little on oxidation. Based on the oxidation potentials of model acetylides and nitriles of both Fe(dppe)Cp and $Ru(PPh_3)_2Cp$ fragments it seems very likely that initial oxidation of **22** and **23** takes place on the iron centre.

From Eqs. 10 and 11, the difference in free energy and reorganisation energy associated with the redox isomers $\mathbf{[22a/b]}^+$ and $\mathbf{[23a/b]}^+$ can be calculated ($\mathbf{[22a/b]}^+$ $\Delta G = 4{,}500$ cm$^{-1}$, $\lambda = 5{,}000$ cm$^{-1}$; $\mathbf{[23a/b]}^+$ $\Delta G = 5{,}700$ cm$^{-1}$, $\lambda = 3{,}500$ cm$^{-1}$). It therefore appears likely that the orientation of the bridge can influence, and perhaps be used to tune, the energetics of the intramolecular electron transfer reaction

## Conclusion

Electrochemical techniques ranging from simple voltammetry to spectroelectrochemical methods provide the key data necessary to assess the thermodynamic and kinetic factors associated with intramolecular electron transfer reactions in bi- and polymetallic systems. When coupled with electronic structure calculations, a detailed insight into the nature of the electron transfer process is obtained. Ethynyl-based bridging ligands are

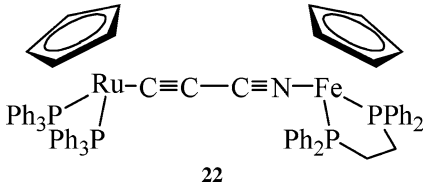

22

**Structure 22**

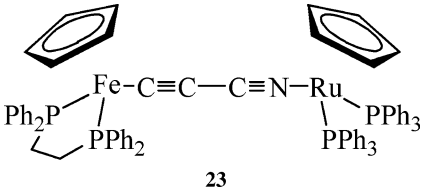

23

**Structure 23**

particularly effective in propagating ground-state delocalisation effects in polymetallic complexes of Group 8 metal systems, while complexes of the heavier metals exhibit stronger couplings in excited states.

## References


1. Allen GC, Hush NS (1967) Prog Inorg Chem 8:357
2. Robin MB, Day P (1967) Adv Inorg Radiochem 10:247
3. Hush NS (1985) Coord Chem Rev 64:135
4. Prassides K (ed) (1991) Mixed valency systems—applications in chemistry, physics and biology. Kluwer, Dordrecht
5. Crutchley RJ (1994) Adv Inorg Chem 41:273
6. Astruc D (1995) Electron transfer and radical processes in transition metal chemistry. VCH, New York
7. Ward MD (1995) Chem Soc Rev 24:121
8. Ceccon A, Santi S, Orian L, Bisello A (2004) Coord Chem Rev 248:683
9. Long NJ, Williams CK (2003) Angew Chem Int Ed 42:2586
10. Osella D, Milone L, Nervi C, Ravera M (1995) J Organomet Chem 488:1
11. Bruce MI, Low PJ (2004) Adv Organomet Chem 50:179
12. Kingsborough RP, Swager TM (1999) Prog Inorg Chem 48:123
13. Lang H (1994) Angew Chem Int Ed Engl 33: 547
14. Lang H, George DSA, Rheinwald G (2000) Coord Chem Rev 206:101
15. Bunz UHF, Rubin Y, Tobe Y (1999) Chem Soc Rev 28:107
16. Bard A, Faulkner LR (1980) Electrochemical methods: fundamentals and applications. Wiley, New York
17. Cruetz C (1983) Prog Inorg Chem 30:1
18. Brunschwig BS, Cruetz C, Sutin N (2002) Chem Soc Rev 31:168
19. Richardson DE, Taube H (1984) Coord Chem Rev 60:107
20. Demanis KD, Hartshorn DC, Meyer TJ (2001) Chem Rev 101:2655
21. Nelson SF (2000) Chem Eur J 6:581
22. Mines GA, Roberts JA, Hupp JT (1992) Inorg Chem 31:125
23. Vance FW, Stone RV, Stern CL, Hupp JT (2000) Chem Phys 253:313
24. Szeghalmi AV, Erdmann M, Engel V, Schmitt M, Amthor S, Kriegisch V, Nöll G, Stahl R, Lambert C, Leusser D, Stalke D, Zabel M, Popp J (2004) J Am Chem Soc 126:7834
25. Coropceanu V, Malagoli M, André JM, Brédas JL (2001) J Chem Phys 115:10409
26. Salaymeh F, Berhane S, Yusof R, de la Rosa R, Fung EY, Matamoros R, Lau KW, Zheng Q, Kober EM, Curtis JC (1993) Inorg Chem 32:3895
27. Hush NS (1967) Prog Inorg Chem 8:391
28. Badger B, Brocklehurst B (1970) Trans Faraday Soc 66:2939
29. Low PJ, Bruce MI (2002) Adv Organomet Chem 48:71
30. Mochida T, Yamazaki S (2002) J Chem Soc Dalton Trans 3559
31. Lavanda C, Bechgaard K, Cowan DO (1976) J Org Chem 41:2700
32. Adams RD, Qu B, Smith MD, Albright TA (2002) Organometallics 21:2970
33. McAdam CJ, Brunton JJ, Robinson BH, Simpson J (1999) J Chem Soc Dalton Trans 2487
34. Adams RD, Qu B, Smith MD (2002) Organometallics 21:3867
35. Jutzi P, Kleinebekel B (1997) J Organomet Chem 545–546:573
36. Levanda C, Cowan DO, Leitch C, Bechgaard K (1974) J Am Chem Soc 96:6788
37. McManis GE, Gochev A, Nielson RM, Weaver MJ (1989) J Phys Chem 93:7733
38. Delgado-Pena F, Talham DR, Cowan DO (1983) J Organomet Chem 253:C43
39. Powers MJ, Meyers TJ (1978) J Am Chem Soc 100:4393
40. Kramer JA, Hendrickson DN (1980) Inorg Chem 19:3330
41. Altmann M, Friedrich J, Beer F, Reuter R, Enkelmann V, Bunz UHF (1997) J Am Chem Soc 119:1472
42. Adams RD, Qu B, Smith MD (2002) Organometallics 21:3867
43. Adams RD, Qu B, Smith MD (2002) Organometallics 21:4847
44. Adams RD, Qu B, Smith MD, Albright TA (2002) Organometallics 21:2970
45. Adams RD, Qu B, Smith MD (2001) Inorg Chem 40:2932
46. Adams RD, Qu B (2000) Organometallics 19:2411
47. Adams RD, Qu B, Smith MD (2001) J Organomet Chem 637–639:514
48. Adams RD, Qu B (2001) J Organomet Chem 619:271
49. Adams RD, Qu B (2001) J Organomet Chem 620:303
50. Adams RD, Qu B (2000) Organometallics 19:4090
51. Adams RD, Qu B (2000) Organometallics 19:2411
52. Bruce MI, Skelton BW, White AH, Zaitseva NN (2002) J Organomet Chem 650:188
53. Bruce MI, Zaitseva NN, Skelton BW, White AH (2002) J. Chem Soc Dalton Trans 1678
54. Champeil E, Draper SM (2001) J Chem Soc Dalton Trans 1440
55. Koridze AA, Zdanovich VI, Lagunova VYu, Petukhova II, Dolgushin FM (2000) Russ Chem Bull 49:1321
56. Duffy N, McAdam J, Nervi C, Osella D, Ravera M, Robinson B, Simpson J (1996) Inorg Chim Acta 247:99
57. McAdam JC, Duffy NW, Robinson BH, Simpson J (1996) Organometallics 15:3935
58. Yam VWW, Fung WKM, Wong KMC, Lau VCY, Cheung KK (1998) Chem Commun 777
59. For lead references see Fox MA, MacBride JAH, Peace RJ, Wade K (1998) J Chem Soc Dalton Trans 401
60. Fox MA, Paterson MAJ, Nervi C, Galeotti F, Puschmann H, Howard JAK, Low PJ (2001) Chem Commun 1610
61. Osella D, Milone L, Nervi C, Ravera M (1998) Eur J Inorg Chem 1473
62. Le Guennic B, Costuas K, Halet JF, Nervi C, Paterson MAJ, Fox MA, Roberts RL, Albesa-Jove D, Puschmann H, Howard JAK, PJ Low (2004) Comp Rendus Chem 2005, DOI:10.1016/j.crci.2005.03.016
63. Wedge TJ, Herzog A, Huertas R, Lee MW, Knobler CB, Hawthorne MF (2004) Organometallics 23:482
64. Chawdhury N, Long NJ, Mahon MF, Ooi L, Raithby PR, Rooke S, White AJP, Williams DJ, Younas M (2004) J Organomet Chem 689:840
65. Thomas KRJ, Lin JT, Wen YS (2000) Organometallics 19:1008
66. Wong WY, Lu GL, Ng KF, Choi KH, Lin Z (2001) J Chem Soc Dalton Trans 3250
67. Wong WY, Ho KY, Choi KH (2003) J Organomet Chem 670:17
68. Wong WY, Lu GL, Ng KF, Wong CK, Choi KH (2001) J Organomet Chem 637-639:159
69. Zhu Y, Wolf MO (2000) J Am Chem Soc 122:10121
70. Engtrakul C, Sita LR (2001) Nano Lett 1:541
71. Field LD, George AV, Laschi F, Malouf EY, Zanello P (1992) J Organomet Chem 435:347
72. Lavastre O, Plass J, Bachmann P, Gusemi S, Moinet C, Dixneuf PH (1997) Organometallics 16:184
73. Beljonne D, Colbert MCB, Raithby PR, Friend RH, Bredas JL (1996) Synth Met 81:179
74. Le Narvor N, Lapinte C (1995) Organometallics 14:634
75. Colbert MCB, Lewis J, Long NJ, Raithby PR, Younus M, White AJP, Williams DJ, Payne NN, Yellowlees L, Beljonne D, Chawdhury N, Friend RH (1998) Organometallics 17:3034
76. Hurst SK, Cifuentes MP, McDonagh AM, Humphrey MG, Samoc M, Luther-Davies B, Asselberghs I, Persoons A (2002) J Organomet Chem 642:259
77. Back S, Lutz M, Spek AL, Lang H, van Koten G (2001) J Organomet Chem 620:227
78. Hurst SK, Ren T (2002) J Organomet Chem 660:1
79. Le Narvor N, Toupet L, Lapinte C (1995) J Am Chem Soc 117:7129

80. Le Stang S, Paul F, Lapinte C (2000) Organometallics 19:1035
81. Roué S, Lapinte C, Bataille T (2004) Organometallics 23:2558
82. Kaim W, Kasack V (1990) Inorg Chem 29:4696
83. Roberts RL (2005) Electrochemical and structural studies of organometallic acetylide complexes, PhD Thesis, University of Durham
84. Le Guennic B (2002) Composés organométalliques et inorganométalliques: Etude théorique des relations structure – nombre d'électrons, Thèse pour le grade de Doctuer de L'Université de Rennes 1
85. Fink H, Long MJ, Martin AJ, Opromolla G, White AJP, Williams DJ, Zanello P (1997) Organometallics 16:2646
86. Flanagan JB, Margel S, Baird AJ, Anson FC (1978) J Am Chem Soc 100:4248
87. Long NJ, Martin AJ, de Biani FF, Zanello P (1998) J Chem Soc Dalton Trans 2017
88. Long NJ, Martin AJ, White AJP, Williams DJ, Fontani M, Laschi F, Zanello P (2000) J Chem Soc Dalton Trans 3387
89. Weyland T, Lapinte C, Frapper G, Calhorda MJ, Halet JF, Toupet L (1997) Organometallics 16:2024
90. Weyland T, Costuas K, Toupet L, Halet JF, Lapinte C (2000) Organometallics 19:4228
91. Weyland T, Costuas K, Mari A, Halet JF, Lapinte C (1998) Organometallics 17:5569
92. Weyland T, Ledoux I, Brasselet S, Zyss J, Lapinte C (2000) Organometallics 19:5235
93. Hurst SK, Cifuentes MP, Humphrey MG (2002) Organometallics 21:2353
94. Bonvoisin J, Launay JP, Van der Auweraer M, De Schryver FC (1994) J Phys Chem 98:5053
95. Osella D, Gobetto R, Nervi C, Ravera M, D'Amato R, Russo MV (1998) Inorg Chem Commun 1:239
96. Jones SC, Coropceanu V, Barlow S, Kinnibrugh T, Timofeeva T, Brédas JL, Marder SR (2004) J Am Chem Soc 126:11782
97. Khan MS, Mandhury MRA, Al-Suti MK, Al-Battashi FR, Al-Saadi S, Ahrens B, Bjernemose JK, Mahon MF, Raithby PR, Younis M, Chawdhury N, Kohler A, Marseglia EA, Tedesco E, Feeder N, Teat SJ (2004) Dalton Trans 2377
98. Khan MS, Al-Suti MK, Mandhury MRA, Ahrens B, Bjernemose JK, Mahon MF, Male L, Raithby PR, Friend RH, Kohler A, Wilson JS (2003) Dalton Trans 65
99. Khan MS, Mandhury MRA, Al-Suti MK, Ahrens B, Mahon MF, L Male, Raithby PR, Boothby CE, Kohler A (2003) Dalton Trans 74
100. Khan MS, Mandhury MRA, Al-Suti MK, Feeder N, Nahar S, Kohler A, Friend RH, Wilson PJ, Raithby PR (2002) J Chem Soc Dalton Trans 2441
101. Khan MS, Mandhury MRA, Al-Suti MK, Hisahm AK, Raithby PR, Ahrens B, Mahon MF, Male L, Marseglia EA, Tedesco E, Friend RH, Kohler A, Feeder N, Teat SJ (2002) J Chem Soc Dalton Trans 1358
102. Bruce MI, Halet JF, Le Guennic B, Skelton BW, Smith ME, White AH (2003) Inorg Chim Acta 350:175
103. Jones ND, Wolf MO, Giaquinta DM (1997) Organometallics 16:1352
104. Zhu Y, Clot O, Wolf MO, Yap GPA (1998) J Am Chem Soc 120:1812
105. Colbert MCB, Lewis J, Long NJ, Raithby PR, White AJP, Williams DJ (1997) J Chem Soc Dalton Trans 99
106. Lebreton C, Touchard D, LePichon L, Daridor A, Toupet L, Dixneuf PH (1998) Inorg Chim Acta 272:188
107. Belen'kaya AG, Dolgushin FM, Peterleitner MG, Petrovskii PV, Krivykh VV (2002) Russ Chem Bull 51:170
108. Sato M, Shintate H, Kawata Y, Sekino M, Katada M, Kawata S (1994) Organometallics 13:1956
109. Sato M, Iwai A, Watanabe M (1999) Organometallics 18:3208
110. Bruce MI, de Montigny F, Jevric M, Lapinte C, Skelton BW, Smith ME, White AH (2004) J Organomet Chem 689:2860
111. Berry JF, Cotton FA, Lu TB, Murillo CA, Roberts BK, Wang XP (2004) J Am Chem Soc 126:7082
112. Berry JF, Cotton FA, Lei P, Lu T, Murillo CA (2003) Inorg Chem 42:3534
113. Xu GL, DeRosa MC, Crutchley RJ, Ren T (2004) J Am Chem Soc 126:3728
114. Xu G, Ren T (2001) Organometallics 20:2400
115. Yip JHK, Wu J, Wong KY, Ho KP, Pun CSN, Vittal JJ (2002) Organometallics 21:5292
116. Hore LA, McAdam CJ, Kerr JL, Duffy NW, Robinson BH, Simpson J (2000) Organometallics 19:5039
117. Richardson DE, Taube H (1981) Inorg Chem 20:1278
118. Cotton FA, Donohue JP, Murillo CA (2003) J Am Chem Soc 125:5436
119. Berry JF, Cotton FA, Murillo CA (2004) Organometallics 23:2503
120. For closely related work see Sheng T, Appelt R, Comte V, Vahrenkamp H (2003) Eur J Inorg Chem 3731
121. Frosch W, Back S, Köhler K, Lang H (2000) J Organomet Chem 601:226
122. Back S, Pritzkow H, Lang H (1998) Organometallics 17:41
123. Hayashi Y, Osawa M, Wakatsuki Y (1997) J Organomet Chem 542:241
124. Neyhart GA, Hupp JT, Curtis JC, Timpson CJ, Meyer TJ (1996) J Am Chem Soc 118:3724
125. Watzky MA, Macatangay AV, Van Camp RA, Mazzetto SE, Song X, Endicott JF, Buranda T (1997) J Phys Chem 10:8441
126. Younus M, Long NJ, Raithby PR, Lewis J (1998) J Organomet Chem 570:55
127. Wong KMC, Lam SCF, Ko CC, Zhu N, Yam VWW, Roué S, Lapinte C, Fathallah S, Costuas K, Kahlal S, Halet JF (2003) Inorg Chem 42:7086
128. Paul F, Meyer WE, Toupet L, Jiao H, Gladysz JA, Lapinte C (2000) J Am Chem Soc 122:9405
129. Jiao H, Costuas K, Gladysz JA, Halet JF, Guillemot M, Toupet L, Paul F, Lapinte C (2003) J Am Chem Soc 125:9511
130. Low PJ, Rousseau R, Lam P, Udachin KA, Enright GD, Tse JS, Wayner DDM, Carty AJ (1999) Organometallics 18:3885
131. Cordiner RL, Corcoran D, Yufit DS, Goeta AE, Howard JAK, Low PJ (2003) Dalton Trans 3541
132. Smith ME, Cordiner RL, Albesa-Jové D, Yufit DS, Hartl F, Howard JAK, Low PJ (2005) Can J Chem (in press)
133. Denis R, Toupet L, Paul F, Lapinte C (2000) Organometallics 19:4240
134. Laidlaw WM, Denning RG (1994) J Chem Soc Dalton Trans 1987